Proceedings of International Scientific and Technical Conference on
"Problems and Prospects of Innovative Technique and Technology in Agri-Food Chain"
Organized by Tashkent State Technical University, Tashkent, Uzbekistan
International Journal of Innovations in Engineering Research and Technology [IJIERT]
ISSN: 2394-3696, Website: www.ijiert.org, Organized on 24-25 April, 2020

VIS-NIR MULTISPECTRAL FEATURES IN CONJUNCTION WITH ANN FOR PREDICTING BIOCHEMICAL AND MICROS-STRUCTURAL FEATURES OF BEEF MUSCLES

A. Aït-Kaddour[1*], *A.* Dubost[2], *J.M.* Roger[3] and A. Listrat[2]

[1] Université Clermont Auvergne, INRAE, VetAgroSup, UMRF, 89 avenue de l'Europe 63370 Lempdes, France
[2] UMR1213 Herbivores, INRAE, VetAgro Sup, Clermont université, Université de Lyon, 63122 Saint-Genès-Champanelle, France
[3] ITAP, INRAE, Montpellier SupAgro, University Montpellier, Montpellier, France

Abstract. The objective of this study was to determine the possibility of Multispectral Imaging (MSI) recorded in the VIS and NIR electromagnetic regions to predict both composition (in some major components), structure of intramuscular connective tissue (IMCT), proportion of intramuscular lipids (IML) and some characteristic parameters of muscle fibres involved in beef sensory quality. In order to do this, three muscles (*Longissimus thoracis*, *Semimembranosus* and *Biceps femoris*) of three type of animal (Aberdeen Angus, Limousine and Blonde d'Aquitaine) were used. After acquisition of images by MSI and segmentation of their morphological parameters, a back propagation ANN model was applied to predict the muscular components and parameters cited above. The predictive models were validated by an external set of samples and the results presented a reasonable accuracy and are promising (R^2 test > 0.90) for real application.

Key words. multispectral; meat; microstructure; biochemical, MSI features; ANN.

1. Introduction

Due to the different food crisis (mad cow, china-adulterated milk, horse gate….) and mistrust of the consumer in the agro-food industry, the sector needs effective technics to authenticate and to determine food quality during processing. Different technics were proposed and actually used in industry for this purpose. Among those technics, classical spectroscopic techniques (e.g. infrared) can be used to perform in-, on-, or at-line measurements, because they have the advantage of not being in physical contact with food products. This advantage decreases the risks of sample physical alteration or contamination during the measurement particularly for sensitive samples like meat. Those technics are also known to be generally quick, cost-effective, and environmentally safe. Therefore, they can be a remarkably effective alternative to traditional analyzes, that are generally expensive, technically long to implement and requiring a high skilled operator. Among those technics, Multi-Spectral Imaging (MSI) is able to depict both spectral and spatial features of a region of interest (ROI) on samples with high dimensions (i.e., few mm^2 up to 10 cm^2). This possibility provides a higher representative information on the sample because the distribution of biochemical components is generally heterogeneous and not equivalent from one point to another. Compared with hyperspectral imaging, less processing time makes MSI easier to meet the speed requirement of industrial production lines used for online high-throughput screening to assess meat quality [1]. The other advantage of MSI is the possibility to record data at different position in the electromagnetic spectrum [2,3] enabling to collect a very rich information on sample chemicals (i.e. absorption, reflection, fluorescence) in spite of the small number of wavelengths. The potentiality of this technology has been used to authenticate and predict physicochemical parameters of food products, such as cheeses [3,4] and pomegranate fruit [5].

In the field of beef, the variability of composition and structure of the raw meat leads to highly variable quality products. Consumers are demanding a constant high quality. The determination of the quality of the beef meat and the parameters on which it depends are therefore essential to guarantee the consumer a meat of constant quality. The muscle (and therefore meat) are mainly composed of muscle fibers packaged in connective tissue (CT), a three-dimensional network that is formed of two structures (*endomysium* and *perimysium*) commonly known as IntraMuscular CT (IMCT). *Endomysium*, surrounds each muscle fiber individually, *perimysium*, in which are located IntraMuscular Lipids (IML), surrounds groups of muscle fibres. The major components of IMCT are a set of fibrillar collagens (commonly called total collagen) whose fibers and fibrils are linked together by covalent links called cross-links (CLs). This network of fiber and fibril of collagen is wrapped by proteoglycans (PGs) [6]. IMCT structural and biochemical characteristics, muscle fibres and IML are known to be involved in beef sensory quality [7,8]. If MSI has been used to predict total collagen and IML [4,9], this technic has never been used to predict the other muscle characteristics in relationship with beef quality cited above. Contrary to hyperspectral imaging, MSI has little been used in the field of beef meat. However it has been applied and was proven to predict tenderness and mechanical properties [9,10], to discriminate samples according to animal age and muscle type [2,4].

Artificial neural network (ANN) is one of the artificial intelligence tools. The ANN model learns to predict automatically from the data set presented during the training the network processes [11]. A variety of ANN models are available and the most commonly used one is the feed forward multi-layer perceptron (MLP). The feed-forward MLP consists of an input layer, an output layer and one or more hidden layers between them. Each neuron is completely connected to all the neurons in the next layer, but only forward links are

available [12]. MLP uses the back propagation learning algorithm, which aims to specify the best parameters to model the relationship between the input and output variables [13]. ANN, among other data mining techniques, combined with spectral data have been increasingly used in animal science (i.e. detection of mastitis, determination of culling reasons, prediction of lactation milk yield) [14,15]. Nonetheless, as far as we know, the application of these methods in order to predict collagen and IMCT properties is, has far as we know, not available in the literature. Therefore, the objective of this study was to determine the possibility of MSI recorded in the VIS and NIR electromagnetic regions coupled with back propagation ANN to predict both the composition (IML, total and insoluble collagens) and some geometrical parameters of the structure of IMCT (e.g. length and width of both *perimysium* and *endomysium*) and density of muscles fibres.

2. Materials and methods

The study was carried out in compliance with French recommendations and those of the Animal Care and Use Committee of the National Institute of Research for Agriculture, Food and the Environment (INRAE) of Clermont-Ferrand/Theix, France, for the use of experimental animals including animal welfare.

Beef muscles - The experiment was performed on 40 young entire males from three types of animals (Aberdeen Angus (AA) (n=12), Limousine (LI) (n=14) and Blonde d'Aquitaine (BA) (n=14) and three muscles (*Longissimus thoracis* (LT), *Semimembranosus* (SM) and *Biceps femoris* (BF)) from each animal in order to create variability. The conditions of production of animals and preparation of samples for structural, biochemical analysis and MSI were previously described [16] [2]. At the end of sampling experiment, a total of 120 samples of beef muscles were obtained.

Structural and biochemical features of connective tissue - All the measures were previously described in details [16]. For structural characterization stained cross-sections were analysed by image analysis with two programs developed using the Visilog 6.7 Professional Software (Noesis, Gif-sur-Yvette, France). The binary images obtained with the programs were used to determine the area of the *perimysium* and *endomysium* (both expressed as % of the total image area). The skeletonized images obtained with the programs were used to determine total length of *perimysium* (expressed in $mm.mm^{-2}$). One parameter was calculated for *endomysium*, the length between 2 triple points (total length/triple point number, named unit length and expressed in µm for endomysium) (Fig. 1). For the muscle fibre study, the labelled images obtained with the programs were used to determine the muscle fibre area (expressed in μm^2) and the fibre number per mm^2. For biochemical characterization, total and insoluble collagen contents were determined according to the two procedures [17, 18]. Both for total and insoluble collagen, data were expressed in mg OH-proline (OH-prol) per g of dry matter (mg/g DM). Total proteoglycan (PG) content was determined according to a modified method [19,20]. Data were expressed in µg of chondroitines-4-sulfates (C4S)-GlycoAmino Glycans (GAGs) equivalents per g of DM (µg C4S-GAGs/g DM) and in mg of C4S-GAGs per g of collagen (mg C4S-GAGs/g OH-prol). IML (i.e. Intra Muscular Lipid or total lipid) content (expressed in g/100 g DM) was estimated by near infrared spectroscopy according to the procedure previously described [21]. The statistical parameters (coefficient of determination and standard error of cross-validation) of the prediction model were 0.81 and 1.75, respectively.

Multispectral image of beef muscles - High quality meat samples MSI were recorded with the VideometerLab2® (Videometer A/S, Danemark). The device was equipped with a multi-spectral camera (Point Gray Research, Scorpion SCOR-20SOM, 1200x1200 pixels) that enables to record 19 images per sample in the VIS-NIR region from 405 to 1050 nm (Fig. 2) [3,22]. The calibration of the camera was performed with three plates, a white one for reflectance correction, a dark one for background correction and a doted one for the pixel position calibration. For each muscle and before image acquisition, the samples were defrosted at 4°C in their plastic bag, equilibrated at 20°C in a water bath, and then cut gently into a 6 x 5 x 1.5 cm^3, wiped out by paper towels in order to reduce the effect of reflection due to surface moisture. The samples were then placed in the dark by lowering the hollow sphere of the MSI system on the sample support plate. Each muscle was illuminated successively by strobing the LEDs. Finally, a data cube for each muscle was obtained with 700 pixels in the X axis, 575 pixels in the Y axis (i.e. called image in the rest of the document) and 19 wavelengths in the Z axis (Fig. 2). Two data cubes were recorded per muscle by performing an acquisition on both sides of the muscles, representing after the analysis 240 data cubes or 4,560 images (i.e. 240 x 19).

Image segmentation and morphological object features - The image correction and segmentation were performed by using the image processing toolbox for Matlab software R2013b (The MathWorks, Natick, Massachusetts, USA). Before image segmentation, the contrast of each image (i.e. recorded per wavelength) was highlighted individually by using the contrast-limited histogram equalization (CLAHE) method [23]. The image was then processed in order to perform segmentation that is needed for the extraction of the objects considered as being IMCT. A specific algorithm sequence was developed based on the Prewitt edge detection and mathematical morphology, to target objects, which belong to the IMCT. Different processing operations were used in the algorithm in order to obtain the best IMCT parameters extraction, like erosion, dilatation and threshold (Fig. 1A). After edge detection, the geometrical characteristics of the image objects considered for IMCT were extracted from the binary images. Eight parameters were calculated: area (1),

surface (2), major axis length (3), minor axis length (4), eccentricity (5), orientation (6), solidity (7), extent and perimeter (8). Then a classification of the objects by size in 10 classes (100, 200, 300, 400, 500, 600, 700, 800, 900 and 1000) between the minimum and maximum of the different object parameters were carried out to produce the characteristic histogram frequency parameter of each sample image. After extraction of the histogram frequency of the objects from each image, 10 new data cubes were obtained, one per histogram frequency class. Each cube presenting in one dimension the number of samples (i.e. beef muscles), in the second one the size of the histogram frequency considered (i.e. 100, 200, 300, 400, 500, 600, 700, 800, 900 or 1000 classes), and in the last one the wavelength dimension (i.e. 19 LEDs). The detailed procedure is presented in Fig. 1B and an example of image obtained after segmentation is presented Fig. 2 to demonstrate the performance of the developed segmentation procedure.

Artificial Neural Network design and architecture - The ANN design has been developed using the neural network toolbox of MATLAB software. A multilayer feed forward network was selected while the back propagation training algorithm was applied to train the network. Uploading the entire image to the network would require thousands of components of the vector and, consequently, the same number of input neurons in the generated ANN. The learning process of a network with a large number of input neurons (and similar number of neurons in hidden layers) would require a large number of learning examples, which in turn would increase the requirements for the processing capacity of the computer [24-27]. For this reasons, in the present study, instead of the direct use of the histograms of the extracted morphological objects as input variables in the ANN model, we transformed them into synthetic variables by Partial least square (PLS).

Fig. 1. Details of the schematic sequence for extraction of shape parameters of meat marbling of each MSI (ROI: Region Of Interest)

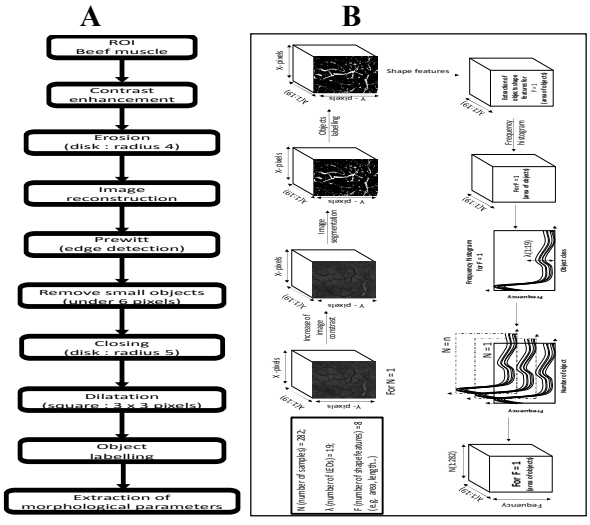

PLS as the advantage to take into account the correlation between the X and Y matrix, while extracting the latent variables (LV) from the X matrix. By the way, the LV directly refer to the given component [28] contrary to the principal components analysis (PCA). Before performing PLS, the histograms were normalized (area under the curve=1) and mean centered. Ten LV for each Y parameter to predict were chosen because their gathered more than 90% of X data variability. A feed forward neural network trained by back-propagation was calculated using the nftool in Matlab. Neurons were organized in four layers, one input layer, two hidden layers and one output layer. There were as many input neurons as LV (n=10) and one output neuron. Concerning the two hidden layers different network were tested varying the number of neurons from 2 to 8 in each hidden layer and testing each possible combination (8 x 8=64). Moreover, the different number of training epochs (from 0 to 1000) were tested. In the training sequence, the output of the network was compared to known values and errors were back-propagated to the hidden and input layers to adjust the weights and minimize the root mean squared error step by step using the method of Levenberg-Marquardt. The procedure was repeated until the errors between the output and known values were minimized. Before performing PLS-ANN, the initial data set was subdivided in 3 data tables, a training dataset containing 70% of the observations (n=168), a validation data set containing 15 % of the observations (n=36), and a testing dataset containing the remaining data (n=36). The data division was performed randomly by using the function dividerand provided in the nftool for Matlab.

Fig. 2. *Biceps femoris* MSI recorded at 450 nm before and after segmentation procedure.

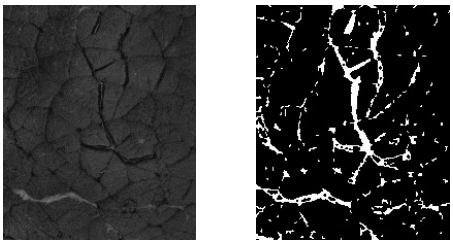

Muscle image at 450 nm Muscle image at 450 nm after segmentation

In order to assess the performance of the models calculated, the determination coefficients in calibration (R^2C), validation (R^2V), and prediction (R^2P), and their corresponding mean square errors in calibration (MSEC), validation (MSEV), and prediction (MSEP) were calculated. In details, R^2 indicates the proportion of the variance in the predicted variable (Y) that can be explained by the variance in the independent variable (X), and the values of RMSEC, RMSECV, RMSEP evaluate the fitting degree of regression during calibration, cross-validation, and prediction. Generally speaking, a robust model should have higher values of R^2C, $R^2V$and R^2P as close as one, and lower values of RMSEC, RMSEV and RMSEP as close as zero [29].

3. Results and discussion

Data sets - Table 1 presented the biochemical and microstructure characteristics of the muscles. These results were previously presented and discussed in detail [16]. Briefly, it was noted that the variation was larger for the total lipids content and finally the collagen contents. More specifically, the total collagen content of the tested muscles varied from 2.94 to 10.45 mg OH-prol/g DM, while the insoluble content varied from 2.01 to 6.87 mg OH-prol/g DM. The max and min values obtained for total lipids varied from 3.61 to 22.82 mg/100 gDM respectively. For the muscles microstructure characteristics, it can be observed that the variation of *perimysium* features is larger than the other microstructural parameters. These results are coherent with previous investigation [6] reporting that perimysial collagen of muscle ranged from 0.45% to 4.76%, whereas endomysial collagen varied from 0.47% to 1.20%. For the microstructure characteristics, the samples presented a *perimysium* with an average area varying from 3.79 to 16.06%, a length varying from 9.38 to 34.61 mm/mm^2. For the endomysium, the average area exhibited values from 3.12 to 10.16% and an average length varying from 2.42E-2 to 3.55 mm. For the fibre density, we noted a min and max values of 202.9 to 441.78 number/mm2.

ANN results - The ANN statistics corresponding to the best models are summarized in Table 1. The critical step for an accurate regression model is to select the optimum number of factors (i.e. epoch, neurons …) needed to calculate the best model. In the present study, in order to select the optimum ANN factors, we firstly identified the optimum numbers giving first local minimum for the RMSEP for each histogram frequency classes (i.e. 100 to 1000). Secondly, the different models based on each histogram frequency were compared and the best one was chosen based on the lowest RMSEP factor.

Table 1. Best ANN results obtained for structural parameters of intramuscular connective tissue and biochemical features of the beef muscles

Microstructure and biochemical parameters	Min	Max	Mean	SD*	CV* (%)	Number classes in the histogram	MSI* features	NIL*	N2L*	Epoch	R2C*	R2V*	R2P*	RMSEC*	RMSEV*	RMSEP*
Perimysium area (%)	3.79	16.06	7.96	1.86	23.34	900	Orientation	2	6	10	0.991	0.984	0.987	0.050	0.076	0.058
Perimysium length (mm/mm^2)	9.38	34.61	18.66	3.86	20.69	900	Orientation	2	6	37	0.988	0.989	0.977	0.325	0.286	0.286
Perimysium width (mm)	0	5.1E-3	4.24E-3	2.72E-4	6.41	900	Orientation	6	8	12	0.966	0.957	0.985	0.000	4.17E-09	3.04E-09
Endomysium area (%)	3.12	10.16	5.82	1.00	17.23	900	Orientation	8	8	53	0.991	0.989	0.984	0.015	0.018	0.018
Length of *endomysium* (mm)	2.42E-2	3.55E-2	3.00E-2	2.09E-3	6.99	900	Orientation	8	2	11	0.984	0.985	0.979	1.01E-07	8.18E-08	8.11E-08
Endomysium width (mm)	1.14	2.8	1.94	0.30	15.44	900	Orientation	8	6	13	0.992	0.991	0.992	0.001	0.001	0.001
Fibre density	202.9	441.78	308.43	43.32	14.04	800	Orientation	2	4	20	0.985	0.973	0.981	46.487	55.397	34.278
Total collagen (mg OH-prol/g DM*)	2.94	10.45	5.59	1.32	23.56	900	Orientation	6	6	44	0.992	0.994	0.992	0.021	0.024	0.023
Insoluble collagen (mg OH-prol/g DM*)	6.87		3.74	0.83	22.24	900	Orientation	6	4	6	0.991	0.985	0.993	0.009	0.017	0.007
IML* Total lipids (mg/100 g DM)	2.01	22.82	7.60	3.00	39.43	900	Orientation	6	4	13	0.992	0.987	0.993	0.111	0.140	0.103

*OH-prol: hydroxy-proline; DM: dry matter; PGs: proteoglycans; GAG: glycosaminoglycanes; coll: collagen; IML: intra muscular lipids; SD: Standard deviation; CV: coefficient of variation (%); MSI: Multispectral image; N1L and N2L: number of neurons in the first and second layer; R2C: R2V: R2P: Coefficient of correlation for prediction; RMSEC: Root Mean Square Error of calibration; RMSEV: Root Mean Square Error of validation; RMSEP: Root Mean Square Error of Prediction; MSI: Multispectral Image.

A global overview of the results highlighted that all the ANN models were accurate because R^2P are higher than 0.96. Moreover, the MSI feature enabling to reach this result are the orientation when considering the 900 or 800 histogram frequency. Considering the prediction for IML, the regression model giving the best ANN model exhibited a R^2P=0.993 and RMSEP=0.103. Our results were more accurate; when compared to Ballerini et al. [30] that also used a segmentation algorithm of muscle from fat developed based on their characteristics in the three-dimensional color space. A correlation value of 0.788 was obtained between chemical analysis and fat percentage computed by image segmentation. The calibration model of Abouelkaram, *et al.* [31] (R^2CV= 0.86), presented also lower accuracy. This difference can be related to the small number of excitation light sources used to record muscle images and to the low variability in their muscle database. Indeed, during they study, they used only three excitation light sources (white Xenon lamp and UV lights at 320 and 380 nm) on BF muscles coming from 6 animals. Nonetheless, in another study El Jabri et al. [9] using equivalent excitation light sources on a higher sample database reported also lower accuracy after cross-validation (R^2CV=0.76). The database included only SM muscle. Moreover, the muscles were withdraw from two breeds, Salers (n=12) and Holstein (n=12) cull cows. In another study, Du, *et al.* [32] reported, after cross-validation, a R^2=0.69, when considering fifty steaks withdrawn from one muscle (*Longissimus dorsi*) on four breeds, Charolais cross-breed, pure Charolais, AA, and Belgian Blue. The steak images were captured on four fluorescent lamps with plastic light diffusers and a polarizer, and were saved in three-dimensional RGB (red, green, and blue) color space. Those results suggested that performance of our predictive models can be certainly explained by the method (ANN) used. Indeed the aforementioned studies used MLR or PLS-R that are more adapted to give models with a good accuracy when a linear relationship exist between the X and Y data. It is established that ANN are generally more accurate for modeling none linear relationship between X and Y. Nonetheless, the segmentation procedure performed on the MSI, in the present study, can also have its importance in the accuracy of the models. Considering the total collagen content, the best model presented a R^2P=0.992 with a RMSEP=0.023. This model was calculated with 6 neurons both in the first and second layer of the ANN. Compared to our results, El Jabri et al. [9] and Abouelkaram et al. [31] reported lower accuracy for the total collagen, R^2=0.74 and 0.86 respectively. For insoluble collagen, the best predictive model gave a R^2P=0.993 and a RMSEP=0.007. Compared to total collagen, the ANN model for soluble collagen was

obtained with a lower number of neurons in the second layer (4 vs 6) and a lower number of epochs (6 vs 44). The best predictive accuracy reported in the present study for total collagen when compared to the literature can be assigned to the same factors aforementioned for the IMF: *(i)* a high database variability by considering three types of animals (LI, BA, and AA) and three muscles types (LT, SM, and BF); *(ii)* differences in excitation lights (i.e., visible and NIR vs Xenon lamp and UV); *(iv)* differences in segmentation algorithms used for spectral image processing. Considering the perimysium and endomysium geometrical features, area, length and width, the best predictive models gave a R^2P higher than 0.96 suggesting a good accuracy. Concerning the prediction of the microstructure of muscle fibres (i.e. density), the ANN models presented R^2P value of 0.981.

Because no previous investigation was reported in the literature, this study brings new insight concerning the prediction of both total, insoluble collagen and microstructure characteristics of the endomysium, perymisum (e.g., area, length, …) and fibre density of beef muscle by using MSI technic. The results reported are promising due to the high R^2P values and since those muscle characteristics can be related to meat tenderness. Indeed, a potential role of the perimysial thickness on tenderness was reported by different authors [33-35]. For example in raw pork [34,35] a positive relationship between perimysial thickness and shear force (R^2= 0.96 and 0.56, respectively) was found. Dubost et al. [7] also reported a negative, contribution of *perimysium* and *endomysium* surface areas in tenderness. This was principally assigned to their denaturation during cooking of meat. For endomysium it was reported that it is thermally denatured at around 50°C, whereas the perimysium was denatured around 65°C [36]. Nonetheless, some contradictory results were reported [33].

4. Conclusion

This work highlighted for the first time the potential of a VIS-NIR multispectral imaging technology combined with ANN analysis to predict both chemical and microstructural characteristics of meat. This was performed in order to propose in long term, a non-destructive, fast and low cost technique to implement for the meat industry. This study also highlighted that a spectral signature in meat sample do exist that can be related to the microstructure characteristic of meat and that multispectral imaging can gather subtle physical and chemical features of this product. The results reported presented a reasonable accuracy and are very promising because evaluating those characteristics can be a good way to replace conventional method. Finally, we hope that this nondestructive emerging technology could be used in a long term as a non-cheaper method in (i) fundamental research on beef muscle and (ii) industry in order to evaluate at an early stage the meat quality, enabling a better process control due to its ease to put in-line.

References

1. Ma, F.; Qin, H.; Shi, K.; Zhou, C.; Chen, C.; Hu, X.; Zheng, L. Feasibility of combining spectra with texture data of multispectral imaging to predict heme and non-heme iron contents in pork sausages. *Food chemistry* **2016**, *190*, 142-149.
2. Aït-Kaddour, A.; Jacquot, S.; Micol, D.; Listrat, A. Discrimination of beef muscle based on visible-near infrared multi-spectral features: Textural and spectral analysis. *International Journal of Food Properties* **2017**, *20*, 1391-1403.
3. Jacquot, S.; Karoui, R.; Abbas, K.; Lebecque, A.; Bord, C.; Aït-Kaddour, A. Potential of Multispectral Imager to Characterize Anisotropic French PDO Cheeses: A Feasibility Study. *International Journal of Food Properties* **2015**, *18*, 213-230.
4. Kulmyrzaev, A.; Bertrand, D.; Lepetit, J.; Listrat, A.; Laguet, A.; Dufour, E. Potential of a custom-designed fluorescence imager combined with multivariate statistics for the study of chemical and mechanical characteristics of beef meat. *Food chemistry* **2012**, *131*, 1030-1036,
5. Khodabakhshian, R.; Emadi, B.; Khojastehpour, M.; Golzarian, M.R.; Sazgarnia, A. Development of a multispectral imaging system for online quality assessment of pomegranate fruit. *International Journal of Food Properties* **2017**, *20*, 107-118.
6. Purslow, P.P. Intramuscular connective tissue and its role in meat quality. *Meat Sci.* **2005**, *70*, 435-447.
7. Dubost, A.; Micol, D.; Picard, B.; Lethias, C.; Andueza, D.; Bauchart, D.; Listrat, A. Structural and biochemical characteristics of bovine intramuscular connective tissue and beef quality. *Meat Science* **2013**, *95*, 555-561.
8. Listrat, A.; Lebret, B.; Louveau, I.; Astruc, T.; Bonnet, M.; Lefaucheur, L.; Picard, B.; Bugeon, J. How muscle structure and composition influence meat and flesh quality. *The Scientific World Journal* **2016**, *2016*, 1-14.
9. El Jabri, M.; Abouelkaram, S.; Damez, J.L.; Berge, P. Image analysis study of the perimysial connective network, and its relationship with tenderness and composition of bovine meat. *Journal of Food Engineering* **2010**, *96*, 316-322.
10. Abouelkaram, S.; Chauvet, S.; Strydom, P.; Bertrand, D.; Damez, J.-L. *Muscle Study with Multispectral Image Analysis*; 2006; pp. 669-670.
11. Dongre, V.B.; Gandhi, R.S.; Singh, A.; Ruhil, A.P. Comparative efficiency of artificial neural networks and multiple linear regression analysis for prediction of first lactation 305-day milk yield in Sahiwal cattle. *Livestock Science* **2012**, *147*, 192-197.
12. Benkrinah, S.; Benslama, M. Acquisition of PN sequences using multilayer perceptron neural network adaptive processor for multiuser detection in spread-spectrum communication systems. *International Journal of Numerical Modelling: Electronic Networks, Devices and Fields* **2018**, *31*, e2265.
13. Fernandez, C.; Soria, E.; Sanchez-Seiquer, P.; Gómez-Chova, L.; Magdalena, R.; Martín-Guerrero, J.D.; Navarro, M.; Serrano, A. Weekly milk prediction on dairy goats using neural networks. *Neural Computing and Applications* **2007**, *16*, 373-381.
14. Gandhi, R.S.; Raja, T.V.; Ruhil, A.P.; Kumar, A. Artificial Neural Network versus Multiple Regression Analysis for Prediction of Lifetime Milk Production in Sahiwal Cattle. *Journal of Applied Animal Research* **2010**, *38*, 233-237.
15. Shahinfar, S.; Mehrabani-Yeganeh, H.; Lucas, C.; Kalhor, A.; Kazemian, M.; Weigel, K.A. Prediction of breeding values for dairy cattle using artificial neural networks and neuro-fuzzy systems. *Comput Math Methods Med* **2012**, *2012*, 127130-127130.
16. Dubost, A.; Micol, D.; Meunier, B.; Lethias, C.; Listrat, A. Relationships between structural characteristics of bovine

intramuscular connective tissue assessed by image analysis and collagen and proteoglycan content. *Meat science* **2013**, *93*, 378-386.
17. Woessner, J.F., Jr. The determination of hydroxyproline in tissue and protein samples containing small proportions of this imino acid. *Arch. Biochem. Biophys.* **1961**, *93*, 440-447.
18. Hill, F. The solubility of intramuscular collagen in meat animals of various ages. *J. Food Sci.* **1966**, *31*, 161-166.
19. Barbosa, I.; Garcia, S.; Barbier-Chassefiere, V.; Caruelle, J.P.; Martelly, I.; Papy-Garcia, D. Improved and simple micro assay for sulfated glycosaminoglycans quantification in biological extracts and its use in skin and muscle tissue studies. *Glycobiology* **2003**, *13*, 647-653.
20. Farndale, R.W.; Sayers, C.A.; Barrett, A.J. A direct spectrophotometric micro-assay for sulfated glycoaminoglycans in cartilage cultures. *Connect. Tissue Res.* **1982**, *9*, 247-248.
21. Guy, F.; Prache, S.; Thomas, A.; Bauchart, D.; Andueza, D. Prediction of lamb meat fatty acid composition using near-infrared reflectance spectroscopy (NIRS). *Food Chem.* **2011**, *127*, 1280-1286.
22. Monson, F.; Sanudo, C.; Sierra, I. Influence of cattle breed and ageing time on textural meat quality. *Meat science* **2004**, *68*, 595-602.
23. Zuiderveld, K. *Contrast Limited Adaptive Histogram Equalization*; 1994; 10.1016/B978-0-12-336156-1.50061-6pp. 474-485.
24. Boniecki, P.; Dach, J.; Pilarski, K.; Piekarska-Boniecka, H. Artificial neural networks for modeling ammonia emissions released from sewage sludge composting. *Atmospheric Environment* **2012**, *57*, 49-54.
25. Boniecki, P.; Nowakowski, K.; Slósarz, P.; Dach, J.; Pilarski, K. Neural image analysis for estimating aerobic and anaerobic decomposition of organic matter based on the example of straw decomposition. In Proceedings of Fourth International Conference on Digital Image Processing (ICDIP 2012); p. 83342B.
26. Boniecki, P.; Nowakowski, K.; Tomczak, R.; Kujawa, S.; Piekarska-Boniecka, H. The application of the Kohonen neural network in the nonparametric-quality-based classification of tomatoes. In Proceedings of Fourth International Conference on Digital Image Processing (ICDIP 2012); p. 833427.
27. Slósarz, P.; Stanisz, M.; Boniecki, P.; Przybylak, A.; Lisiak, D.; Ludwiczak, A. Artificial neural network analysis of ultrasound image for the estimation of intramuscular fat content in lamb muscle. *African Journal of Biotechnology* **2011**, *10*, 11792.
28. Preda, I.; Jodal, U.; Sixt, R.; Stokland, E.; Hansson, S. Normal Dimercaptosuccinic Acid Scintigraphy Makes Voiding Cystourethrography Unnecessary after Urinary Tract Infection. *The Journal of Pediatrics* **2007**, *151*, 581-584.e581.
29. Cheng, C.-H.; Nührenberg, G.; Ruess, H. Maximum resilience of artificial neural networks. In Proceedings of International Symposium on Automated Technology for Verification and Analysis; pp. 251-268.
30. Ballerini, L.; Hogberg, A.; Lundstrom, K.; Borgefors, G. Color image analysis technique for measuring of fat in meat: an application for the meat industry. In Proceedings of Machine Vision Applications in Industrial Inspection IX; pp. 113-124.
31. Abouelkaram, S.; Berge, P.; Hocquette, J.F.; Culioli, J.; Listrat, A. Image analysis study of the relationship between total collagen content and distribution of the perimysial connective network in a bovine muscle. *Sciences des Aliments* **2003**, *23*, 166-170.
32. Du, C.-J.; Sun, D.-W.; Jackman, P.; Allen, P. Development of a hybrid image processing algorithm for automatic evaluation of intramuscular fat content in beef M. longissimus dorsi. *Meat Sci.* **2008**, *80*, 1231-1237.
33. Brooks, J.C.; Savell, J.W. Perimysium thickness as an indicator of beef tenderness. *Meat Sci.* **2004**, *67*, 329-334.
34. Fang, S.H.; Nishimura, T.; Takahashi, K. Relationship between development of intramuscular connective tissue and toughness of pork during growth of pigs. *J. Anim. Sci.* **1999**, *77*, 120-130.
35. Nishimura, T.; Fang, S.; Wakamatsu, J.-I.; Takahashi, K. *Relationships between physical and structural properties of intramuscular connective tissue and toughness of raw pork*; 2009; Vol. 80, pp. 85-90.
36. Li, C.B.; Zhou, G.H.; Xu, X.L. Dynamical changes of beef intramuscular connective tissue and muscle fiber during heating and their effects on beef shear force. *Food Bioprocess Technol.* **2010**, *3*, 521-527.